

## A Stable High-Index Surface of Silicon: Si(5 5 12)

A. A. Baski, S. C. Erwin, L. J. Whitman\*

A stable high-index surface of silicon, Si(5 5 12), is described. This surface forms a  $2 \times 1$  reconstruction with one of the largest unit cells ever observed, 7.7 angstroms by 53.5 angstroms. Scanning tunneling microscopy (STM) reveals that the 68 surface atoms per  $2 \times 1$  unit cell are reconstructed only on a local scale. A complete structural model for the surface is proposed, incorporating a variety of features known to exist on other stable silicon surfaces. Simulated STM images based on this model have been computed by first-principles electronic-structure methods and show excellent agreement with experiment.

As the basis for a multibillion-dollar industry, the surfaces of silicon are the most widely studied of all semiconductors. Despite such scrutiny, only three stable surfaces of clean silicon have generally accepted structural models: the well-known low-Miller index (001) and (111) planes and the high-index (113) plane (1-3). As is common for covalently bonded materials, all of these clean surfaces reconstruct in order to reduce the energy associated with their surface dangling bonds. On Si(001), the surface atoms pair up as dimers to form a  $2 \times 1$  reconstruction. On Si(111), a number of different reconstructions are observed, including the metastable  $2 \times 1$  structure with the top two surface layers rearranged into  $\pi$ -bonded chains (observed on a cleaved surface), and the equilibrium  $7 \times 7$  structure with a more complicated dimer-adatom-stacking fault (DAS) structure (observed after cooling from high temperatures). High-index Si(113), a surface consisting of alternating rows of atoms with (001) and (111) orientation, is stabilized by a  $3 \times 2$  reconstruction composed of re-bonded and dimerlike step edge atoms. Sub-

strates oriented to (110), (331), and (015) also appear to have stable surfaces, but their structures have not been well established (4-7).

Although Si(001) is the dominant substrate for electronic device fabrication, high-index surfaces are being investigated as possible substrates for specialized applications (8-10). An ideally structured high-index surface (that is, bulk-terminated) would consist of a periodic array of low-index terraces separated by steps of monatomic height. Such a surface would provide a natural template for the growth of one-dimensional structures (8) and high-quality heteroepitaxial films (9, 10). However, the actual surface morphologies on high-index surfaces are usually not ideal, because of the influence of surface reconstructions, step and kink energies, and step-step interactions. In general, these surfaces may consist of a distribution of low-index terraces separated by variable-height steps or step bunches, or in the extreme case, may break up (facet) into planes of different orientations (11).

Whereas Si surfaces tilted only a few degrees away from (001) and (111) have been well characterized, less is known about high-index surfaces tilted farther away from these planes. Given the established stability of Si(113), which is oriented nearly midway between (001) and (111), high-index sur-

A. A. Baski and L. J. Whitman, Code 6177, Naval Research Laboratory, Washington, DC 20375, USA.  
S. C. Erwin, Code 6691, Naval Research Laboratory, Washington, DC 20375, USA.

\*To whom correspondence should be addressed.

Report Documentation Page				Form Approved OMB No. 0704-0188	
Public reporting burden for the collection of information is estimated to average 1 hour per response, including the time for reviewing instructions, searching existing data sources, gathering and maintaining the data needed, and completing and reviewing the collection of information. Send comments regarding this burden estimate or any other aspect of this collection of information, including suggestions for reducing this burden, to Washington Headquarters Services, Directorate for Information Operations and Reports, 1215 Jefferson Davis Highway, Suite 1204, Arlington VA 22202-4302. Respondents should be aware that notwithstanding any other provision of law, no person shall be subject to a penalty for failing to comply with a collection of information if it does not display a currently valid OMB control number.					
1. REPORT DATE <b>1995</b>		2. REPORT TYPE		3. DATES COVERED <b>00-00-1995 to 00-00-1995</b>	
4. TITLE AND SUBTITLE <b>A Stable High-Index Surface of Silicon: Si(5 5 12)</b>				5a. CONTRACT NUMBER	
				5b. GRANT NUMBER	
				5c. PROGRAM ELEMENT NUMBER	
6. AUTHOR(S)				5d. PROJECT NUMBER	
				5e. TASK NUMBER	
				5f. WORK UNIT NUMBER	
7. PERFORMING ORGANIZATION NAME(S) AND ADDRESS(ES) <b>Naval Research Laboratory, Code 6177, 4555 Overlook Avenue SW, Washington, DC, 20375</b>				8. PERFORMING ORGANIZATION REPORT NUMBER	
9. SPONSORING/MONITORING AGENCY NAME(S) AND ADDRESS(ES)				10. SPONSOR/MONITOR'S ACRONYM(S)	
				11. SPONSOR/MONITOR'S REPORT NUMBER(S)	
12. DISTRIBUTION/AVAILABILITY STATEMENT <b>Approved for public release; distribution unlimited</b>					
13. SUPPLEMENTARY NOTES					
14. ABSTRACT					
15. SUBJECT TERMS					
16. SECURITY CLASSIFICATION OF:			17. LIMITATION OF ABSTRACT <b>Same as Report (SAR)</b>	18. NUMBER OF PAGES <b>5</b>	19a. NAME OF RESPONSIBLE PERSON
a. REPORT <b>unclassified</b>	b. ABSTRACT <b>unclassified</b>	c. THIS PAGE <b>unclassified</b>			

faces oriented between these two low-index planes are of particular interest (Fig. 1). It is known that Si(001) surfaces tilted only a few degrees toward (111) consist of (001) terraces separated by single atomic-height steps, whereas at higher tilt angles ( $\approx 2^\circ$  to  $5^\circ$ ) double-height steps occur (12). Similarly, Si(111) surfaces tilted up to  $12^\circ$  toward (001) form (111) $7 \times 7$  terraces separated by both single-height and triple-height steps, with the fraction of triple-height steps increasing with increasing angle (13, 14). Recently, we found that at even higher tilt angles ( $>14^\circ$ ) the triple-height steps are replaced by (337)-like terraces separated by (111) $7 \times 7$  terraces that are one unit cell wide, resulting in the formation of quasi-periodic sawtoothlike nanofacets on the surface (15). This result provided evidence for the existence of a stable surface near (337). After examining planar surfaces near this orientation, we have discovered another stable surface of silicon, Si(5 5 12), which we now describe.

These experiments were performed in ultrahigh vacuum (UHV) with Si wafers oriented to within  $1^\circ$  of (5 5 12) and cleaned as described previously (15). After cleaning, the samples were cooled slowly ( $\approx 2^\circ\text{C}$  per second) from  $\approx 1150^\circ\text{C}$  to room temperature to obtain the equilibrium surface structure. Atomic-resolution scanning tunneling microscopy (STM) topographs of both the filled and empty electronic states were acquired with a constant current between 0.1 and 0.3 nA and bias voltages between 1.0 and 2.5 V.

Scanning tunneling microscopy images of the clean (5 5 12) surface display a well-ordered, periodic arrangement of row struc-

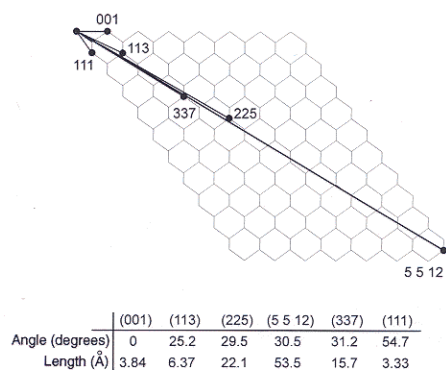


**Fig. 1.** Side view of a Si crystal lattice bounded by the (001) and (111) planes. The intersections of the lattice lines represent projections of atomic positions onto the  $\{110\}$  plane (the plane of the page). Six plane orientations on this lattice are indicated by line segments, with the length of each line equaling one unit cell of the associated bulk-terminated surface. The crystal truncation of one unit cell of (5 5 12) is equivalent to that of two unit cells of (337) plus one of (225). The table lists the angle with respect to the (001) plane and the bulk-terminated unit cell length for each orientation.

tures oriented along the  $[\bar{1}10]$  direction (Fig. 2). The period of this structure in the  $[6\bar{6}5]$  direction is  $\approx 54 \text{ Å}$ , equal to the length of the bulk-terminated (5 5 12) unit cell. In Fig. 3, the topography of the filled electronic states is displayed along with top and side views of the bulk-terminated (5 5 12) surface. As shown, each unit cell of the bulk-terminated (5 5 12) surface is equivalent to two unit cells of (337) plus one unit cell of (225) (Figs. 1 and 3), that is, the atoms at the surface are the same in either case. The excellent correspondence between the STM topography and the lengths of the (337) and (225) subunits confirms that the observed surface has a (5 5 12) orientation. In addition, the topography of each of these units is identical to that observed on structures unambiguously identified as (337)

and (225) unit cells in a previous study (15). This clearly demonstrates that Si(5 5 12) is a stable surface (16) and is reconstructed only on a local scale within the constituent (337) and (225) units.

The atomic-scale topography of the filled electronic states on the Si(5 5 12) surface is dominated by three types of row structures having specific locations with respect to each other (Fig. 3A). The most prominent rows on the surface (labeled "a") are the primary rows. These rows define the (225) and (337) subunits and consist of oblong maxima with a bulk-like  $a_0$  period along  $[\bar{1}10]$  ( $a_0 = 3.84 \text{ Å}$ ). Within each unit of (225), there are two internal rows: secondary ("b") and tertiary ("c"). The blocklike secondary rows always occur to the right (that is, toward  $[6\bar{6}5]$ ) of the typically zigzag-shaped tertiary rows. In con-

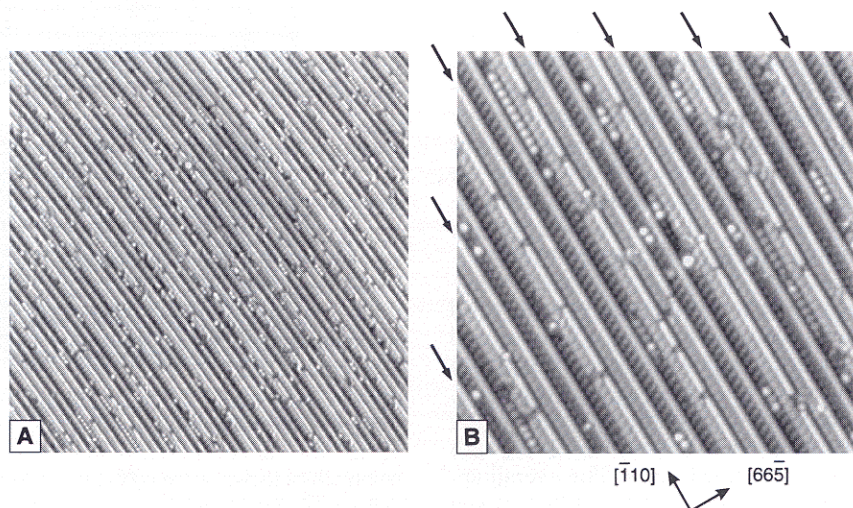
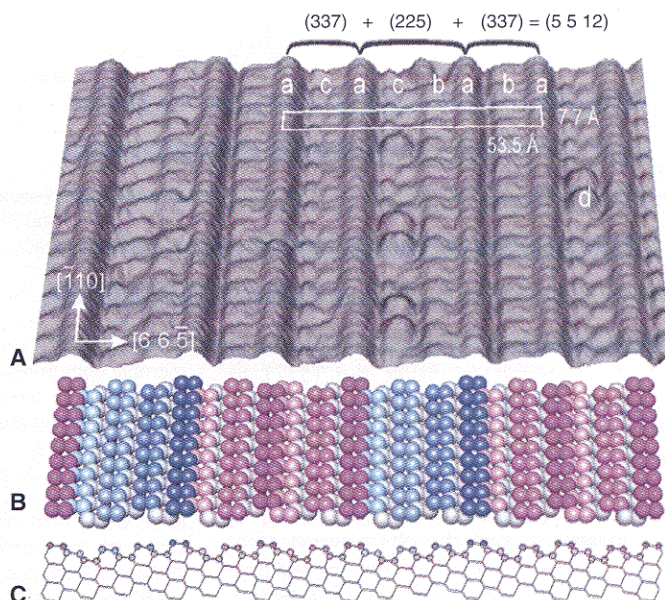


**Fig. 2.** Filled-state STM gray-scale images of Si(5 5 12): (A)  $\approx 750 \text{ Å}$  by  $750 \text{ Å}$  (4.6 Å height range); (B)  $\approx 300 \text{ Å}$  by  $300 \text{ Å}$  (4.3 Å height range). Arrows indicate the surface periodicity.

**Fig. 3.** (A) Rendered  $120 \text{ Å}$  by  $115 \text{ Å}$  image of Si(5 5 12) (3.0 Å height range). One unit cell of the  $2 \times 1$  reconstruction is outlined. Labels denote the following surface structures: (a) primary rows, (b) secondary rows, (c) tertiary rows, and (d) ad-dimer. (B) Top view of a model bulk-terminated Si(5 5 12) surface. (C) Side view of the bulk-terminated structure. As indicated, each unit cell of the (5 5 12) surface can be described as two unit cells of (337) (pink-purple) plus one of (225) (blues).



trast, each unit of (337) has only one internal row, which is a secondary row if the (337) unit is to the right of a (225) unit, and a tertiary row if it is to the left. In addition to the row structures, protrusions ("d") are occasionally observed, but only on top of the tertiary rows. The secondary and tertiary rows both have a  $2a_0$  period along  $[\bar{1}10]$ ; hence, the (5 5 12) surface has a  $2 \times 1$  reconstruction with a unit cell of  $7.7 \text{ \AA}$  by  $53.5 \text{ \AA}$ .

Because STM images are a convolution of both physical and electronic structure, it is important to examine the topography of both the filled and empty electronic states on surfaces of covalently bonded materials such as Si. Figure 4 shows atomic-resolution images of both of these states acquired simultaneously on the same area of a (5 5 12) surface. Each of the structures discussed previously has a unique signature in such dual-bias images that provides important clues to the underlying atomic structure. For example, each protrusion on the tertiary rows appears as one maximum in the filled-state image, but as two maxima (oriented either parallel or perpendicular to the rows) in the empty-state image. This dual-bias behavior is similar to that observed for Si dimers (ad-dimers) adsorbed on Si(001) (17), strongly suggesting a similar dimer structure here.

The dual-bias behavior of the row structures is more complicated. As described above, the primary rows have an  $a_0$  period corrugation along the  $[\bar{1}10]$  row direction in the filled states. In the empty states, a similar corrugation is visible, but the oblong maxima are out of phase along  $[\bar{1}10]$  with respect to the filled states. The overall appearance and phase relationship between the filled and empty states of the primary rows resemble that of the  $\pi$ -bonded rows observed on cleaved Si(111) $2 \times 1$  (18). In contrast to the primary rows, both the secondary and tertiary rows have a  $2a_0$  period along  $[\bar{1}10]$  and appear substantially different in the filled-state versus empty-state images. The secondary rows have a block-like appearance in the filled states and an asymmetric structure in the empty states with a node along the center line; these features are similar to the tetramers seen on reconstructed Si(113) (2, 3). In contrast to the consistent structure of the primary and secondary rows, the internal structure of the tertiary rows shows considerable variation, especially in the filled states. Two common structures, found in either the (337) or (225) units, are symmetrical pairs [see (337) tertiary row in Fig. 4] and zigzags [see (225) tertiary row]. In the empty states, the tertiary rows are more uniform and appear as a diffuse line slightly off center.

On the basis of the characteristic features observed in dual-bias images, we propose a model of the (5 5 12) $2 \times 1$  surface

that can be constructed from a few simple structural units:  $\pi$ -bonded chains, dimers, and tetramers. Figure 5 illustrates the proposed structure of the primary, secondary, and tertiary rows as incorporated into the (225) subunit of the (5 5 12) $2 \times 1$  surface. In our proposed model, the primary row is a  $\pi$ -bonded chain situated atop six-member rings, a variation of the  $\pi$ -bonded chains found atop seven-member rings on the

Si(111) $2 \times 1$  surface (19). Note that this  $\pi$ -bonded chain changes the stacking arrangement of the surface atoms from unfaulted on the left to faulted on the right. To the right, the primary rows are connected to five-member rings with no dangling bonds, which are in turn connected to seven-member rings with another  $\pi$ -bonded chain on top. Directly adjacent to this second  $\pi$ -bonded chain is a dimer-chain wall

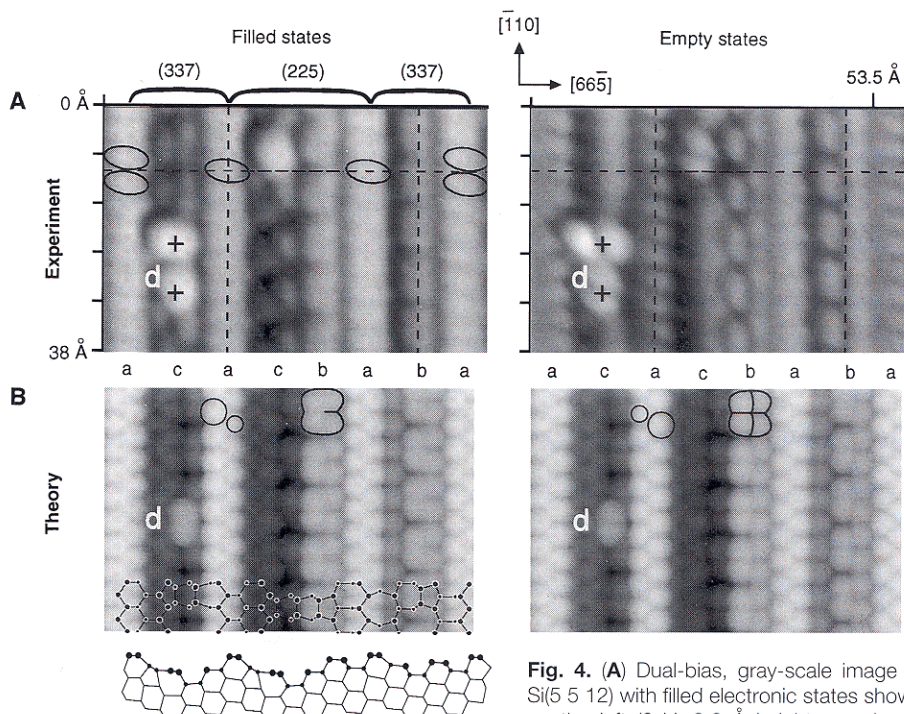
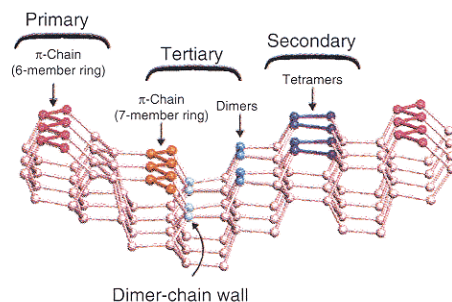


**Fig. 4.** (A) Dual-bias, gray-scale image of Si(5 5 12) with filled electronic states shown on the left (2 V, 3.6 Å height range) and empty states shown on the right (1 V, 4.4 Å height range). These images have been corrected for thermal drift. Labels denote the following surface structures: (a) primary rows, (b) secondary rows, and (c) tertiary rows. Crosses mark the approximate centers of protrusions (d), believed to be adsorbed dimers, which are sometimes observed (with two possible orientations) on the tertiary rows. As reference aids, ovals highlight the maxima along the primary rows in the filled-state image, and dashed lines are drawn at identical locations in both images. Note that as a natural consequence of the diamond crystal structure, the corrugation of the primary rows along  $[\bar{1}10]$  is out of phase across the (337) subunit but in phase across (225). (B) Simulated filled- and empty-state images of a proposed model for the (5 5 12) $2 \times 1$  surface ( $\approx 5 \text{ \AA}$  height range). One ad-dimer (d) oriented parallel to  $[\bar{1}10]$  is shown. At the top of both simulated images, features associated with the primary and secondary rows are highlighted. A top view of the model is overlaid on the bottom of the filled-state image. A side view of the model is displayed directly below.

**Fig. 5.** Ball-and-stick model of the (225) subunit of the reconstructed Si(5 5 12) $2 \times 1$  surface. Labels indicate the locations of the primary, secondary, and tertiary rows, as well as key structural elements of the model. Each of the three row structures are associated with specific structural units: primary row =  $\pi$ -bonded chain located atop six-member rings (magenta); secondary row = row of dimer-bonded tetramers (blue-purple); tertiary row =  $\pi$ -bonded chain located atop seven-member rings (orange) + dimer-chain wall (cyan) + row of dimers (blue). Note that the stacking sequence of the surface atoms (with respect to those below) is shifted by both the primary row and the dimer-chain wall: the atoms to the left of the dimer-chain wall are faulted and those to the right are unfaulted. The structures illustrated here can be arranged to form the (337) subunits necessary to model a complete (5 5 12) $2 \times 1$  surface.



that switches the stacking arrangement back to an unfaulted sequence. This wall is analogous to the wall found between the triangular unfaulted and faulted regions on Si(111)7 × 7.

The first structure on the unfaulted side of the (225) subunit is a row of dimers oriented along  $\bar{1}10$ , similar to the dimers found on the Si(001)2 × 1 surface. This dimer row, combined with the neighboring  $\pi$ -bonded chain, accounts for the tertiary row in the STM images. To the right of the tertiary row we find the dimer-bonded tetramers of the secondary row, containing two dimer-bonded atoms (left pair) and two threefold-coordinated atoms (right pair). The structural units (Fig. 5) can be arranged to form the two (337) subunits that complete the (5 5 12)2 × 1 unit cell. Within this unit cell, the 68 bulk-terminated surface atoms are locally rearranged to halve the number of dangling bonds per 2 × 1 unit cell from 48 to 24 (20).

Our model of the Si(5 5 12)2 × 1 surface is strongly supported by idealized theoretical simulations of the filled- and empty-state STM images. First-principles electronic-structure methods were used to calculate the local state density at position  $\mathbf{r}$  and energy  $\epsilon$

$$\rho(\mathbf{r}, \epsilon) = \sum_{\mathbf{n}, \mathbf{k}} |\Psi_{\mathbf{n}, \mathbf{k}}(\mathbf{r})|^2 \delta(\epsilon - \epsilon_{\mathbf{n}, \mathbf{k}}) \quad (1)$$

where  $\mathbf{r}$  is a distance vector and  $\Psi_{\mathbf{n}, \mathbf{k}}(\mathbf{r})$  is the self-consistent wave function for band  $n$ , wave vector  $\mathbf{k}$ , and energy  $\epsilon_{\mathbf{n}, \mathbf{k}}$ . The calculations were performed within the local-density approximation (LDA) to density-functional theory by an all-electron method with a local-orbital basis set (21). To approximate constant-current STM images, we generated simulated images by finding the height  $z$  above the surface for which the integrated local state density  $\int \rho(\mathbf{r}, \epsilon) d\epsilon$  is constant, with the integral taken over filled or empty states within 2 eV of the Fermi level (22). The resulting images are shown in Fig. 4 (23).

In general, the correspondence between the simulated and experimental images is excellent, both with respect to the lateral positions of the features and their relative heights (see Fig. 4). In the simulated images, the  $\pi$ -bonded chains of the primary rows appear as asymmetric zigzag chains with the expected  $a_0$  period along  $\bar{1}10$ . As anticipated (23), the individual maxima along the chains are better resolved in the calculated images than in the STM data, appearing as two circular maxima as opposed to one oblong maximum. The maxima are more pronounced on the left side of the chains in the filled states, and vice versa in the empty states, reproducing the out-of-phase condition observed in the STM images (24). In the secondary rows, the internal structure and relative height with re-

spect to the primary rows are also in good agreement. In the filled states, the tetramers result in a blocklike shape strongly resembling the STM data; in the empty states, a thin nodal line along  $\bar{1}10$  occurs in the center of the row, in reasonable agreement with experiment.

The tertiary rows are relatively more complicated because of their variable appearance in the STM data. This variation has a natural origin in the row of dimers on the right side of the tertiary row. Because dimers on Si(001)2 × 1 are found in both flat and buckled configurations, we assume that both occur on the (5 5 12) surface as well. Additionally, we assume that the dimer chain wall in the center of the tertiary row induces a weak  $2a_0$  periodicity in the adjacent  $\pi$ -bonded chain to the left. For flat dimers, this perturbation consists of a small dimerization of the chain atoms, whereas for buckled dimers, it leads to a small buckling of the chain atoms. We find that the simulated filled-state image qualitatively reproduces the features seen in the data of Fig. 4 if the dimers are flat in this particular (337) subunit and buckled in the (225) subunit.

Additional support for our model comes from consideration of possible ad-dimer adsorption sites. An ad-dimer of either orientation can be easily accommodated in the tertiary row, between the  $\pi$ -bonded chain and the dimer row, with bond lengths that are close to ideal. No such adsorption site is available elsewhere on the model surface, consistent with the experimental observation that ad-dimers are found only on the tertiary rows. We have calculated the topography associated with a periodic array of dimers adsorbed on a (337) tertiary row and incorporated one unit cell of the simulated image into Fig. 4.

The idealized theoretical simulations strongly support our proposed model of the Si(5 5 12)2 × 1 surface. Simulated images for alternative models, for example, rebonded step edge arrangements (25), significantly differ from the STM images. We therefore conclude that this model is essentially correct, with the possible exception of some minor relaxations of the atomic positions. A precise theoretical determination of the structure would require an ab initio total energy calculation with all atoms allowed to move freely, a formidable task given that there are 68 atoms per 2 × 1 layer. To put this problem into perspective, such a calculation for the simpler Si(111)7 × 7 DAS reconstruction (49 atoms per 7 × 7 layer) has only recently been possible with massively parallel algorithms and hardware (26, 27).

The most remarkable aspect of the Si(5 5 12)2 × 1 reconstruction may be that it involves only a local rearrangement of the 68 surface atoms in each 2 × 1 unit

cell. It is very unusual for a high-index surface to have an equilibrium structure so close to its bulk termination; the resultant unit cell is one of the largest ever observed, 7.7 Å by 53.5 Å. The stability of the surface can be in part attributed to its low density of dangling bonds (dbs). In our model of the 2 × 1 reconstruction, this density is 0.058 dbs/Å<sup>2</sup>, a value between that for Si(001)2 × 1 (0.068 dbs/Å<sup>2</sup>) and Si(111)7 × 7 (0.030 dbs/Å<sup>2</sup>). If the dangling bond density were the only criteria, however, then we would expect the tertiary (337) unit cells (which have a lower density, 0.050 dbs/Å<sup>2</sup>) to form a stable planar surface—contrary to our observation (28). We believe that another critical factor is surface stress and that the local stress associated with the (337) and (225) subunits compensate each other within the (5 5 12) unit cell, leading to a surface with net lower energy. Preliminary calculations support this belief, indicating that while both types of (337) units are under compressive stress, the (225) unit is under tensile stress (29).

Reconstructions of semiconductor surfaces are driven by a delicate energy balance between a variety of factors, the most important of which are the elimination of dangling bonds and the minimization of surface stress. Our characterization of Si(5 5 12) demonstrates how the structure of even a complicated semiconductor surface can be understood in terms of a small number of simple building blocks that reduce the number of dangling bonds, provided that the composite structure has a low net strain energy. Only by simultaneous consideration of both dangling bonds and surface stress will progress continue to be made in the understanding of very large-scale semiconductor surface reconstructions. As the feature size on Si-based electronic devices approaches the nanometer scale, such progress will become increasingly important.

## REFERENCES AND NOTES

1. See, for example, R. Becker and R. Wolkow, in *Scanning Tunneling Microscopy*, J. A. Stroscio and W. J. Kaiser, Eds. (Academic Press, San Diego, CA, 1993), pp. 149–224.
2. J. Knall, J. B. Pethica, J. D. Todd, J. H. Wilson, *Phys. Rev. Lett.* **66**, 1733 (1991).
3. J. Dabrowski, H.-J. Müssig, G. Wolff, *ibid.* **73**, 1660 (1994).
4. Y. Yamamoto, *Phys. Rev. B* **50**, 8534 (1994).
5. H. Tanaka, T. Yokoyama, I. Sumita, *Appl. Surf. Sci.* **76–77**, 340 (1994).
6. M. Tomitori, K. Watanabe, M. Kobayashi, F. Iwakaki, O. Nishikawa, *Surf. Sci.* **301**, 214 (1994).
7. A variety of other surfaces have been observed on multifaceted substrates; however, to our knowledge their stability has not been confirmed on oriented planar substrates. See, for example, B. Röttger, M. Hanbücken, I. Vianey, R. Kliebe, H. Neddermeyer, *Surf. Sci.* **307–309**, 656 (1994).
8. T. M. Jung, R. Kaplan, S. M. Prokes, *Surf. Sci.* **289**, L577 (1993).

9. L. Fotiadis and R. Kaplan, *Thin Solid Films* **184**, 415 (1990).
10. P. M. Mooney, F. K. LeGoues, J. Tersoff, J. O. Chu, *J. Appl. Phys.* **75**, 3968 (1994).
11. E. D. Williams and N. C. Bartelt, *Science* **251**, 393 (1991).
12. B. S. Swartzentruber, N. Kitamura, M. G. Lagally, M. B. Webb, *Phys. Rev. B* **47**, 13432 (1993).
13. J. Wei, X.-S. Wang, J. L. Goldberg, N. C. Bartelt, E. D. Williams, *Phys. Rev. Lett.* **68**, 3885 (1992).
14. B. Li, thesis, University of Maryland (1993).
15. A. A. Baski and L. J. Whitman, *Phys. Rev. Lett.* **74**, 956 (1995).
16. Independent evidence for the stability of Si(5 5 12) has recently been found in x-ray scattering measurements: S. Song, M. Yoon, S. G. J. Mochrie, *Surf. Sci.* **334**, 153 (1995).
17. P. J. Bedrossian, *Phys. Rev. Lett.* **74**, 3648 (1995).
18. R. M. Feenstra and J. A. Stroscio, *ibid.* **59**, 2173 (1987).
19. A modest buckling of 0.10 Å was assumed for the  $\pi$ -bonded chain atoms in the primary rows. This buckling is considerably smaller than the 0.45 Å buckling predicted for the Si(111)2  $\times$  1 Pandey  $\pi$ -bonded chain, whose seven-member rings allow for greater structural flexibility. See, for example, J. E. Northrup, M. S. Hybertsen, S. G. Louie, *Phys. Rev. Lett.* **66**, 500 (1991).
20. This calculation assumes that the  $\pi$ -bonded chains reduce the effective number of dangling bonds on the chain by a factor of 2.
21. S. C. Erwin, M. R. Pederson, W. E. Pickett, *Phys. Rev. B* **41**, 10437 (1990).
22. Given the large size of the (5 5 12) unit cell, the following two simplifications were introduced to make the LDA calculation tractable: (i) The simulated images for the (5 5 12) surface were approximated by treating each of the three subunits [(225), (337) with a secondary row, and (337) with a tertiary row] as separate periodic surfaces, then combining the resulting images to form a single composite image. (ii) Structural relaxation was not performed on the entire structure; instead, atomic positions were fixed according to the theoretical local geometries of the proposed structural units.
23. As a result of a number of computational approximations, we expect topographical features in the simulated images to show better resolution and less diffuse character than corresponding features observed in STM images, particularly for the empty states. (i) The approximation of the tunneling matrix element by a constant neglects any role of the tip structure in degrading image resolution. (ii) The low average height  $z \approx 3$  Å in the simulations, approximately half the experimental tip-surface distance, results in more localized features. Note that this height is determined by the chosen integrated local-state density  $n = 10^{-6}$  electrons/bohr<sup>3</sup>, which is constrained by the relatively narrow vacuum region separating adjacent slabs in the calculation. (iii) The relatively small basis set limits the extended nature of the unoccupied conduction states. (iv) The approximation of Brillouin-zone sums by a single point at the zone center ( $k = 0$ ) artificially emphasizes the localization of unoccupied  $\pi$ -bonded surface states, which have antibonding character at the zone center.
24. The symmetry inequivalence of the two atoms on either side of the chain opens a gap in the corresponding surface state, with the occupied bonding combinations favoring the upper chain atom (that is, filled-state maxima are more pronounced to the left) and the antibonding combination favoring the lower chain atom (that is, empty-state maxima are more pronounced to the right).
25. D. J. Chadi, *Phys. Rev. B* **29**, 785 (1984).
26. I. Stich, M. C. Payne, R. D. King-Smith, J.-S. Lin, *Phys. Rev. Lett.* **68**, 1351 (1992).
27. K. D. Brommer, M. Needels, B. E. Larson, J. D. Joannopoulos, *ibid.*, p. 1355.
28. A clean Si(337) surface is composed of (5 5 12) terraces separated by step bunches or short (111)7  $\times$  7 facets.
29. S. C. Erwin, A. A. Baski, L. J. Whitman, unpublished.
30. We are grateful to S. G. J. Mochrie for providing us with results prior to publication. This work was funded by the Office of Naval Research and a Naval Research Laboratory/National Research Council Postdoctoral Fellowship (A.A.B.), and was supported in part by a grant of high-performance computing time from the Department of Defense Shared Resource Center MAUI.

22 May 1995; accepted 3 July 1995